

Peptide Bonds in the Interstellar Medium: Facile Autocatalytic Formation from Nitriles on Water-Ice Grains

Boutheïna Kerkeni^{1,2*†} and John M. Simmie^{3†}

¹ISAMM, Université de la Manouba, Tunisia 2010.

²Faculté des Sciences de Tunis, Laboratoire de Physique de la Matière Condensée, Université Tunis el Manar, Tunisia 2092.

³School of Chemistry, University of Galway, Ireland H91 TK33.

*Corresponding author(s). E-mail(s):

boutheina.kerkeni@isamm.uma.tn;

Contributing authors: john.simmie@nuigalway.ie;

†These authors contributed equally to this work.

Abstract

A recent suggestion that acetamide, $\text{CH}_3\text{C}(\text{O})\text{NH}_2$, could be readily formed on water-ice grains by the acid induced addition of water across the CN bond is now shown to be valid. Computational modelling of the reaction between $\text{R}-\text{CN}$ ($\text{R} = \text{H}, \text{CH}_3$) and a cluster of 32 molecules of water and one H_3O^+ proceeds auto-catalytically to form firstly a hydroxy imine $\text{R}-\text{C}(\text{OH})=\text{NH}$ and secondly an amide $\text{R}-\text{C}(\text{O})\text{NH}_2$. Quantum mechanical tunnelling, computed from small-curvature estimates, plays a key role in the rates of these reactions. This work represents the first credible effort to show how amides can be formed from abundant substrates, namely nitriles and water, reacting on a water-ice cluster containing catalytic amounts of hydrons in the interstellar medium with consequential implications towards the origins of life.

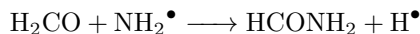
Keywords: amides, ISM, nitriles, quantum chemistry

1 Introduction

The peptide bond, $-\text{C}(\text{O})\text{NH}-$, found in amides connects amino acids to peptides — of paramount importance to present day life on Earth. Unsurprisingly, how, when and where peptide bond formation arose is of immediate interest in prebiotic astrochemistry, tackling that challenging question: the origins of life [1, 2].

The simplest amides, formamide $\text{HC}(\text{O})\text{NH}_2$, and acetamide, $\text{CH}_3\text{C}(\text{O})\text{NH}_2$, are common constituents of star-forming regions in our galaxy [3, 4] but apparently propionamide, $\text{CH}_3\text{CH}_2\text{C}(\text{O})\text{NH}_2$, is not [5]. Adande et al. [3] have shown, based on their observations of formamide towards star-forming regions of dense molecular clouds, that the compound could have been brought to Earth by exogenous delivery in substantial amounts of ~ 0.18 mmol m^{-2} in a single impact.

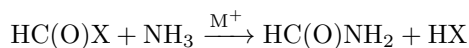
The formation routes to formamide are still unclear; some have suggested gas-phase pathways via formaldehyde and amidogen [6, 7]:



but disputed by Song and Kästner [8] and convincingly refuted by Douglas et al. [9] or surface reactions [10] by the hydrogenation of isocyanic acid, HNCO , and on carbon monoxide-ammonia ices [11]:



and more recently by metal-ion mediated substitution reactions [12]:



where $\text{M} = \text{Na}^+, \text{K}^+, \text{Mg}^+, \text{Mg}^{++}, \text{Al}^+$ and $\text{X} = \text{H}, \text{OH}, \text{CH}_2\text{OH}$ but the evidence for all these is underwhelming. A comprehensive summary has been given recently by Chuang et al. [13] during the course of their laboratory work on the formation of formamide in water- and carbon monoxide-rich water ices with ammonia as the substrate. VUV irradiation of water-rich and CO-rich ammonia ices at 10 K with compositions $\text{H}_2\text{O}:\text{CO}:\text{NH}_3=10:5:1$, $\text{CO}:\text{NH}_3=4:1$ and $\text{CO}:\text{NH}_3=0.6:1$ have shown that formamide is preferentially formed, although mechanistically the situation is complicated with no clear indication as to actual formation routes [13]. Indirect evidence for the formation routes of formamide based on the stratified distribution of the molecules HNCO and H_2CO , putative parents of HCONH_2 , in the atmosphere of the HH 212 protostellar disk appear to rule out HNCO as a parent [14].

Studies of comets have indicated that the early Solar Nebula had nitriles (cyanides) such as HCN and CH_3CN in abundance [15, 16]. It is currently

assumed that reactions in the bulk or on the surface of water-ice grains are the most likely formation routes for complex organic molecules which are then liberated into the gas-phase by UV irradiation, electron and cosmic ray bombardment, via thermal shocks or grain–grain collisions [17, 18, 19].

In a computational study of the direct reaction $\text{HC}\equiv\text{N} + \text{H}_2\text{O} \longrightarrow \text{HC}(\text{OH})=\text{NH}$ neither the presence of a second H_2O as a catalyst, or as a spectator or as a reactant was sufficient to reduce the high barriers encountered which thereby rule out the possibility of it occurring in cold molecular clouds [20]. The most pertinent previous work simulated a 33 H_2O molecule cluster and showed that $\text{HC}\equiv\text{N}$ cannot react to $\text{HC}(\text{O})\text{NH}_2$ under interstellar ice conditions because of large energy barriers. Any reactivity that was feasible proceeded through the CN^\bullet radical [21].

UV photolysis of water methyl cyanide ices at 20 K ($\text{H}_2\text{O}:\text{CH}_3\text{CN} = 20:1$) does give rise to the formation of $\text{CH}_3\text{C}(\text{O})\text{NH}_2$, and its isomer N-methyl formamide CH_3NHCHO , but many other products as well [22].

A consideration of the various suggested reactions in the literature led one of us to suggest that H_3O^+ induced water addition to nitriles on water-ice grains was likely to provide the most probable route [23]. It is known that H_3O^+ exists in the ISM and even in other galaxies, that it reacts in water-ices and that it has the potential to drive subsequent reaction [24, 25, 26, 27]. Woon has very recently reviewed what is known about cation–ice reactions from quantum chemical cluster studies, highlighting the novel and more efficient pathways, vis-à-vis the gas-phase, that HCO^+ , CH_3^+ and C^+ (but not H_3O^+) undergo and appealed for experimental confirmation [28]. Laboratory experiments have shown that bombardment of water ice samples on a copper substrate at 10 K yields a number of secondary ions including $(\text{H}_2\text{O})_n \cdot \text{H}^+$ with $n = 1 \rightarrow 8$, although these ions are perhaps more accurately denoted as $(\text{H}_2\text{O})_{n-1} \cdot \text{H}_3\text{O}^+$ [29]. The production efficiency is much lower when crystalline ice is bombarded in comparison to amorphous ice.

The first step in the proposed addition of water is the protonation at nitrogen of the nitrile to form $\text{RC}\equiv\text{NH}^+$, and in the case of HCN to form imino methylium, $\text{HC}\equiv\text{NH}^+$; this species has been widely detected in star-forming regions [30, 31, 32] and in Titan’s atmosphere [33]. Although it had been characterised as a precursor of $\text{HC}\equiv\text{N}$ in the most recent observations Fontani et al. show that it is formed from $\text{HC}\equiv\text{N}$ or $\text{HC}\equiv\text{N}^+$ [34]. Fundamental laboratory work to characterise the spectroscopic parameters for $\text{CH}_3\text{C}\equiv\text{NH}^+$ have been carried out but interstellar searches have not so far been successful [35].

A primary consideration for suggesting acidified amorphous water-ice is the high mobility of the proton through the lattice; the transfer mechanism, via Grotthuss hops, takes place on a sub-picosecond time scale and with barriers of $\approx 1 \text{ kJ mol}^{-1}$ — these effectively increase the “collision rate” or encounter between reactant and H_3O^+ [27, 36].

The hydronium induced addition of water was seen as a two-step process with the first forming hydroxy imines or imidic acids $\text{RC}(\text{OH})=\text{NH}$ and the second converting these to amides $\text{RC}(\text{O})\text{NH}_2$; the latter reaction can occur

either by intramolecular hydrogen-transfer via quantum-mechanical tunnelling or by the further protonation of the nitrogen-atom followed by deprotonation from the O-atom.

The actual formation of peptides as a by-product was observed [37] after the deposition of C atoms onto a CO + NH₃ ice at 10 K and subsequent warming to 300 K. The authors argue that the initial reaction product is aminoketene, H₂NCH=C=O, which polymerises on warming yielding $(-\text{CH}_2-\text{C}(\text{O})-\text{NH}-)_n$ chains. While the experiments are compelling the conditions are somewhat artificial since they consider pure CO + NH₃ ices with substantial quantities of carbon atoms. The initial step H₃N + C(³P₀) → H₃N-C is highly exothermic, $\Delta_r H = -103 \text{ kJ mol}^{-1}$, this is followed by a 1,2-H-transfer to H₂N-CH and finally reaction with CO to H₂N-CH=C=O.

Interestingly Canepa [38] in considering the survival rates of glycine, NH₂CH₂C(O)OH, embedded in micrometeorites undergoing atmospheric re-entry has shown that aminoketene, the product of dehydration, would also survive.

In this paper we focus on a solid-state chemistry formation mechanism of R-C(OH)=NH and subsequently R-C(O)NH₂. We perform electronic structure investigations of the energetics and also thermal rate constants calculations of this reaction mechanism. This information can then be used in astrochemical modelling and may prompt experimental laboratory confirmation.

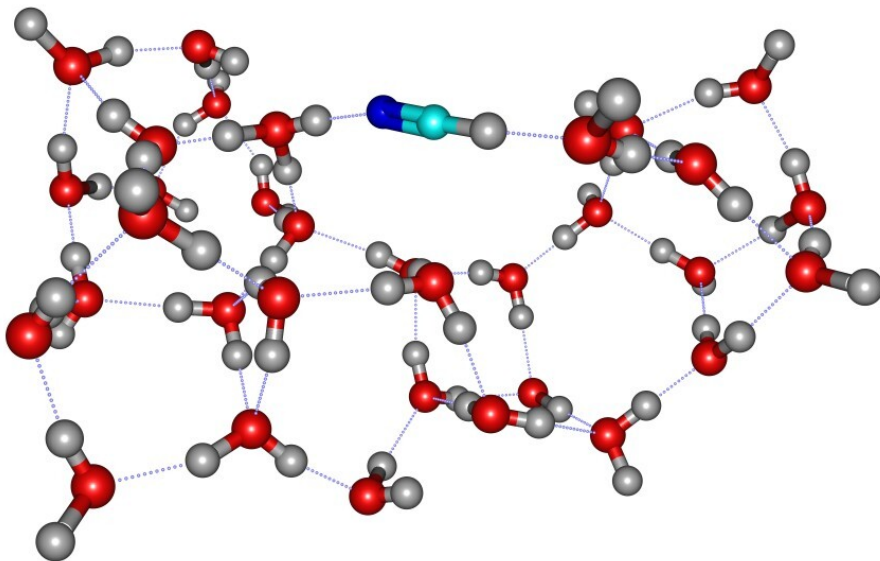


Fig. 1: HCN embedded in acidified water

2 Methods

Calculations were performed with the application Gaussian [39] and used the long-range dispersion corrected hybrid meta-GGA density functional ω B97X-D together with the triple ζ basis set with added polarization and diffuse functions 6-311++G(d,p) [40] with a factor of 0.96 was applied to scale the zero-point energy.

A system with thirty-two water molecules and one hydronium ion, H_3O^+ , with a total ‘volume’ of $\approx 2,600 \text{ \AA}^3$, was chosen together with one reactant, either HCN or CH_3CN . This choice represents a compromise between realistic ISM concentrations and computational effort Fig. 1.

All structures were fully optimized and the harmonic frequencies computed using DFT. Frequency calculations were performed in order to verify that all intermediates are true minima on the potential energy surface, and that all transition states exhibit a single imaginary frequency. We study all species in the reaction mechanism with the unrestricted ω B97XD/6-311++G(d,p) model chemistry. Gaussian 16 automatically includes an ultrafine integration grid in the DFT calculations in order to improve the accuracy of the results. The grid greatly enhances the accuracy at reasonable additional cost.

The reaction paths are computed using the intrinsic reaction coordinate (IRC) methodology [41, 42] to confirm the identities of the reactants and products for every transition state. IRC calculations require initial force constants of the transition state. Then, the first and second order energy derivatives are obtained to calculate the projected harmonic vibrational frequencies along each reaction path. The minimum energy paths (MEPs) were computed using the Page–McIver integrator with a gradient step size of $0.1 a_0$ [43].

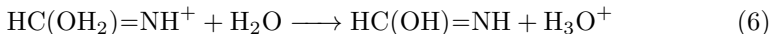
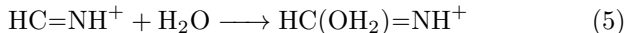
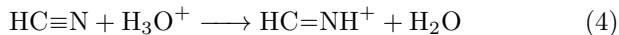
Small curvature quantum mechanical and quantised-reactant-states tunnelling calculations [44, 45] employed the PILGRIM application [46] for the computation of rate constants via transition state theory (TST) and variational TST (VTST) necessitating calculations along the minimum energy path.

3 Results

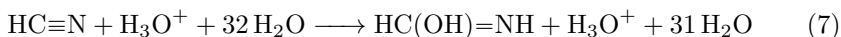
Prior to the first reaction steps we begin by considering a previously published [47] cluster of 33 water molecules, $[33(\text{H}_2\text{O})]$, to which a low energy hydron H^+ is added in a highly exothermic process, $\Delta_r H(0\text{K})$ of $-1,065 \text{ kJ mol}^{-1}$; this in turn can be dissipated throughout the cluster and/or serves to drive subsequent reactions. The only notable difference between the two clusters $[33(\text{H}_2\text{O})]$ and $[33(\text{H}_2\text{O}) \cdot (\text{H}^+)]$, which is more realistically depicted as $[32(\text{H}_2\text{O}) \cdot (\text{H}_3\text{O}^+)]$, are the three additional vibrational modes, two O–H asymmetric stretching vibrations near $2,400 \text{ cm}^{-1}$ and a characteristic symmetric at $2,800 \text{ cm}^{-1}$. It is to this cluster that the reactants HCN and CH_3CN are then added.

3.1 First step: imidic acid formation

As originally envisaged the hydrolysis of $\text{HC}\equiv\text{N}$ proceeded in three distinct phases:



the exothermic first step $\Delta_r H^\ominus(0\text{ K}) = -20.5\text{ kJ mol}^{-1}$ simply a reflection of the larger proton affinity of $\text{HC}\equiv\text{N}$ of 712.9 kJ mol^{-1} vis-à-vis H_2O of 691.0 kJ mol^{-1} [48]. In a water cluster of an additional 32 H_2O molecules however these later steps are elided since as H_2O adds to the C-atom it simultaneously transfers H to a neighbouring O-atom.



Overall reaction (4) is exothermic by -80 kJ mol^{-1} which is considerably different to the gas-phase $\Delta_r H^\ominus(0\text{ K}) = -22.2\text{ kJ mol}^{-1}$ reflecting the tighter binding of the hydrolysed product in comparison to the reactant.

The barrier to reaction (1), that is protonation at the N-atom, in the case of HCN is 78.5 kJ mol^{-1} and is even lower at 51.9 kJ mol^{-1} for acetonitrile.

Although Fig. 1 shows the actual reaction structure, an oversimplified version, Fig. 2, shows the parts played by four key water molecules; the first is the proton donor H_3O^+ , the second is the “reactant” which will attack the C-atom and also transfer a H^+ to the “acceptor” water, whilst the “companion” H_2O is less involved but nevertheless stabilises the system through $\text{H}\cdots\text{OH}_2$ hydrogen-bonding; snapshots along the IRC path are shown in Fig. 3 to the final product, methanimidic acid in its (*E,Z*) conformation with respect to the dihedrals $\angle\text{OCNH}$ and HO CN , respectively.

In Fig. 4 we plot the potential energy along the minimum energy path for the imidic acid formation given by reaction (4).

3.2 Second step: amide formation

We can distinguish between two different routes from the hydroxy imines to the corresponding amides which can proceed intra-molecularly or inter-molecularly.

3.2.1 Intramolecular route

Once the hydroxy imines, methanimidic and ethanimidic acids, are formed then an intra-molecular 1,3-H-transfer leads to formamide, Fig. 5, or acetamide; however, the barriers are considerable ranging from 136 or 128 kJ mol^{-1} in the gas-phase to 169 and 142 kJ mol^{-1} in this water-cluster; clearly, surmounting such barriers is unfeasible at temperatures much less than 300 K except by tunnelling.

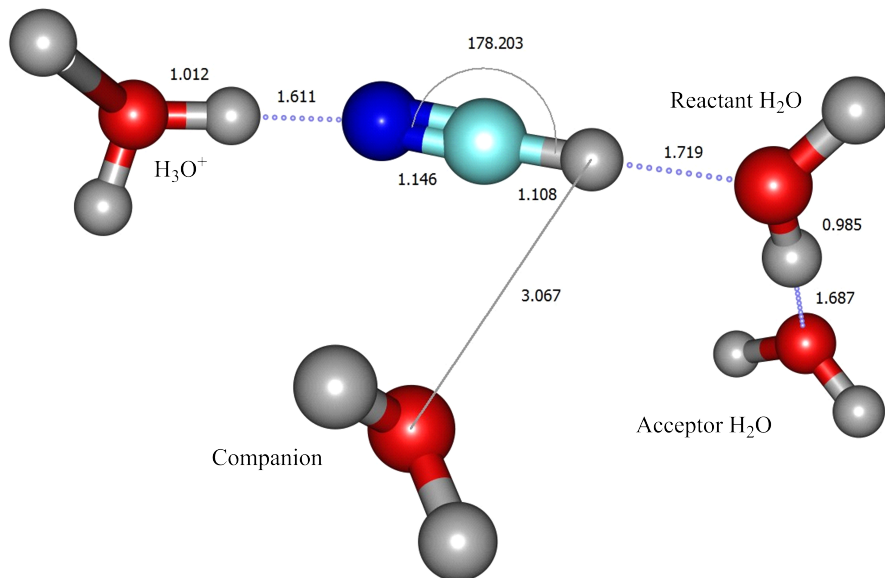


Fig. 2: Key elements of the reaction scheme for the first step

Note that the presence of additional water molecules makes very little difference to the energetics of the process in comparison to the gas-phase. Exactly the same conclusion can be drawn from the gas-phase work of Darla et al. which showed in ω B97xD/aug-cc-pVTZ calculations that even in the presence of a “catalytic” water molecule the 1,3[H]-transfer faces a barrier of 131 kJ mol^{-1} or 132 kJ mol^{-1} with the additional water present as a “spectator” [20].

The additional water molecules and H_3O^+ in our system only marginally affect the 1,3[H]-transfer reaction; this is seen in the energetics, as discussed above, and also from the values of the imaginary frequencies which are gas-phase: $2,002$ and $1,988 \text{ cm}^{-1}$ and cluster: $1,953$ and $1,916 \text{ cm}^{-1}$ for $\text{HC(OH)NH} \leftrightarrow \text{HC(O)NH}_2$ and $\text{CH}_3\text{C(OH)NH} \leftrightarrow \text{CH}_3\text{C(O)NH}_2$ respectively.

In the case of the gas-phase $\text{RC(OH)NH} \leftrightarrow \text{RC(O)NH}_2$ isomerisation reaction, PILGRIM [49] calculations at B3LYP/cc-pVTZ incorporating small-curvature tunnelling yields rate constants, k , and half-lives, τ , as shown in Table 1; the ice-cluster values are probably not dis-similar. At the lowest temperatures, *here* $\leq 150 \text{ K}$, quantised reactant states tunnelling is included. The barrier to reaction is higher at $131.5 \text{ kJ mol}^{-1}$ for HC(OH)NH_2 than the $123.9 \text{ kJ mol}^{-1}$ for $\text{CH}_3\text{C(OH)NH}_2$ consequently the rate of isomerisation to the appropriate amide is faster for ethanimidic acid. These are substantially faster rates of isomerisation than our previous Multiwell values, Fig. 6, which were based on Eckart tunnelling [23]; this renders the intermolecular route, discussed below, essentially redundant.

A not dis-similar situation is considered by Concepción et al [50] in their work on the origin of the (E/Z) isomer ratio of imines in the ISM; thus

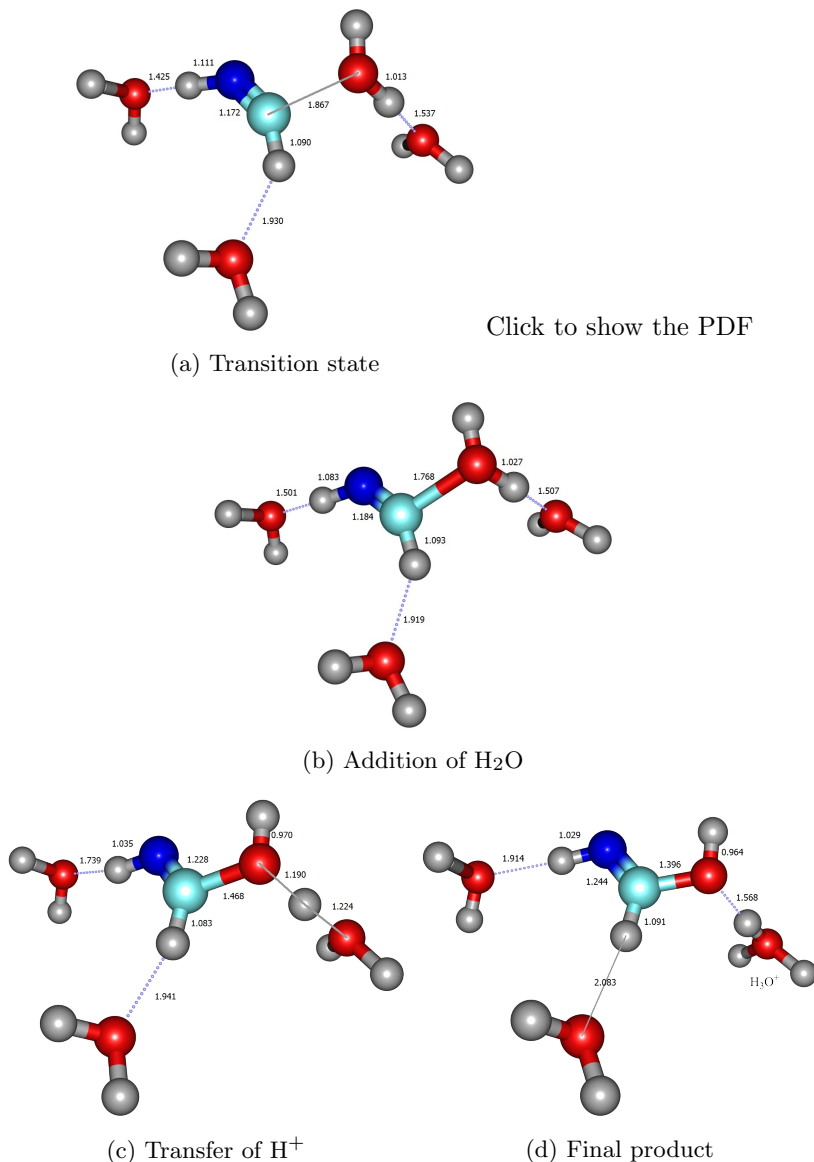


Fig. 3: Structures along the IRC path for the first step

they show that the less-stable (*E*) conformer of cyanomethanimine, RCH=NH where R is a C≡N group, re-arranges to the (*Z*) with dramatically increased rates over canonical transition-state theory values at temperatures of 250 K and below. The variational effect is small and the faster rates are ascribed to quantum tunnelling; exactly the same as found *here*.

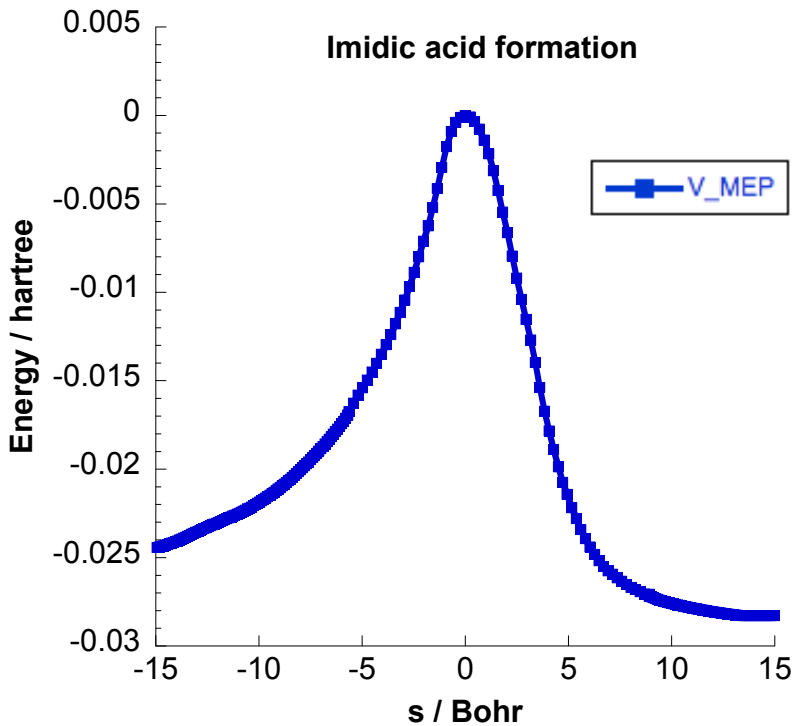


Fig. 4: Classical potential energies V_{MEP} as functions of s / Bohr for imidic acid formation in ice.

T / K	$\text{HC(OH)NH} \rightarrow \text{HC(O)NH}_2$		$\text{CH}_3\text{C(OH)NH} \rightarrow \text{CH}_3\text{C(O)NH}_2$	
	k / s^{-1}	τ / days	k / s^{-1}	τ / days
50	7.6×10^{-09}	1,060	4.4×10^{-08}	180
100	7.8×10^{-09}	1,028	8.3×10^{-08}	100
150	1.2×10^{-08}	660	2.3×10^{-07}	36
200	4.2×10^{-08}	190	9.3×10^{-07}	9
250	3.4×10^{-07}	24	6.7×10^{-06}	2
300	4.4×10^{-06}	2	7.5×10^{-05}	0.2

Table 1: Isomerisation rate constants

The detection of isotopically labelled compounds can be useful for tracing formation routes; specifically, deuteration has been used in this regard by Bianchi et al. [51] in their study of $\text{CH}_3\text{C}\equiv\text{N}$ in the SVS13-A Class I hot corino. Unfortunately, such a tool is unavailable here since the hydrogen transferred has been sourced from the water-ice; however were $\text{CH}_3\text{C(OD)NH}$ or $\text{CH}_3\text{C(OH)ND}$ to be detected then that might prompt other avenues of investigation.

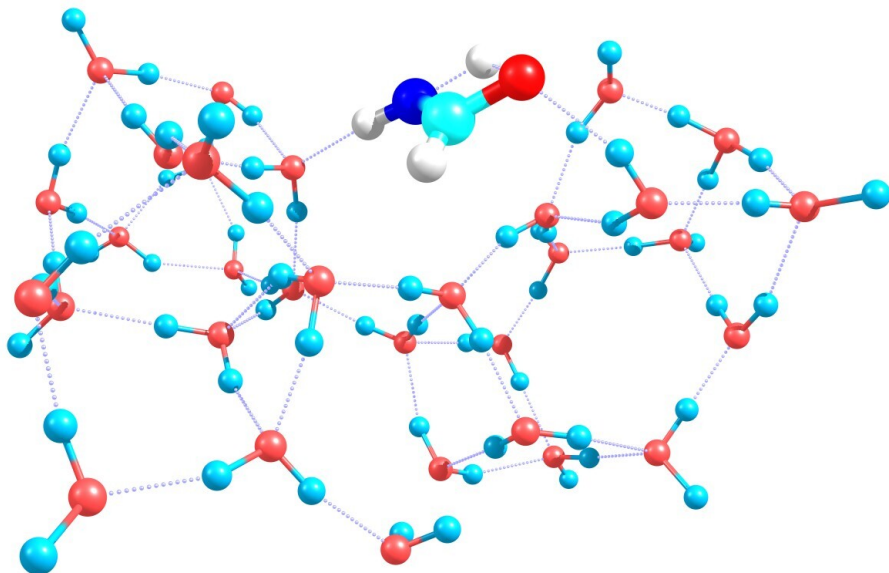


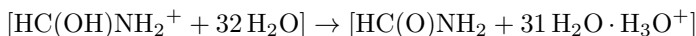
Fig. 5: Transition state for 1,3[H]-transfer; $\text{HC}(\text{OH})\text{NH} \rightarrow \text{HC}(\text{O})\text{NH}_2$

In Fig. 7 we plot the potential energy, the zero point energy (ZPE), and vibrationally adiabatic ground state energy V_a^G along the minimum energy path for the gas phase 1,3-H-transfer.

3.2.2 Intermolecular route

The same outcome, that is $\text{RC}(\text{OH})\text{NH} \rightarrow \text{RC}(\text{O})\text{NH}_2$, can come about by the attack of hydronium at the N-atom leading similarly to $\text{R}-\text{C}(\text{OH})=\text{NH}_2^+ + \text{H}_2\text{O}$ and attack by a further water molecule at the O-atom leading to deprotonation, resulting in the final products $\text{R}-\text{C}(\text{O})-\text{NH}_2 + \text{H}_3\text{O}^+$.

So this reaction follows the same course mechanistically as the first; firstly, protonation at the nitrogen atom, which has a tiny barrier of 1.6 kcal/mol (disappears when adding ZPE), is followed by H-abstraction from the OH group and transfer of H to a neighbouring water and transfer of H to a second water, Fig. 8, which just shows the active site. The reaction can be summarised as:



and the barrier for this is low at 5.8 kJ mol^{-1} . The results are summarised in Table 2 where E^\ddagger is the zero-point corrected electronic energy and $\Delta_r H$ is the reaction enthalpy, with both expressed in units of kJ mol^{-1} .

4 Discussion

There are of course other nitriles present in the ISM and one would anticipate that a similar fate would befall them; Manna and Pal [52] have detected

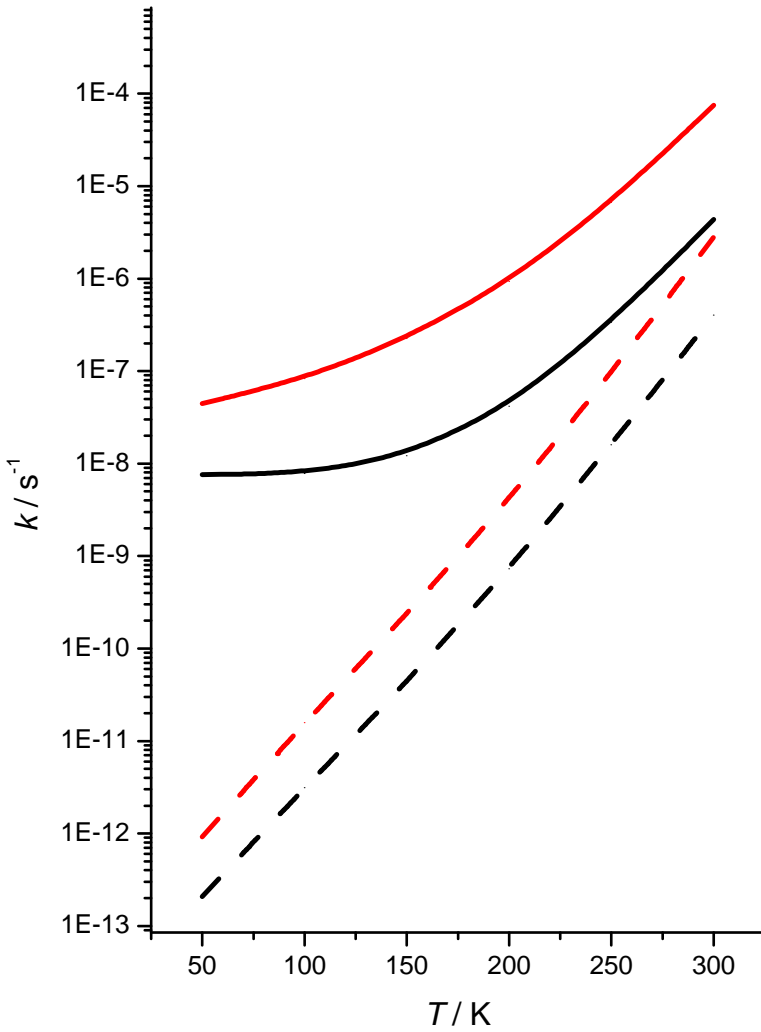


Fig. 6: Rate constants gas-phase isomerisation: Eckart versus small-curvature tunnelling. $\text{CH}_3\text{C}(\text{OH})\text{NH}$, $\text{HC}(\text{OH})\text{NH}$.

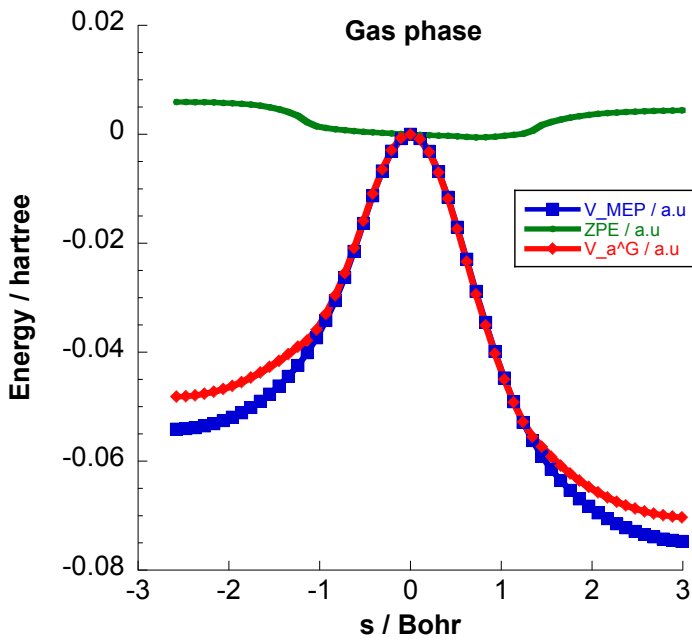


Fig. 7: Classical potential energies V_{MEP} , ground-state vibrational adiabatic potential energy (V_a^G), and ZPE as functions of s / Bohr for 1,3[H]-transfer in gas phase

Reaction	E^\ddagger	$\Delta_r H$ (0 K)
Initial protonation and hydroxy imine formation		
$\text{HCN} + 32 \text{H}_2\text{O} \cdot \text{H}_3\text{O}^+ \rightarrow \text{HCNH}^+ + 33 \text{H}_2\text{O} \rightarrow \text{HC(OH)NH} + 31 \text{H}_2\text{O} \cdot \text{H}_3\text{O}^+$	78.5	-82.8
$\text{CH}_3\text{CN} + 32 \text{H}_2\text{O} \cdot \text{H}_3\text{O}^+ \rightarrow \text{CH}_3\text{CNH}^+ + 33 \text{H}_2\text{O} \rightarrow \text{CH}_3\text{C(OH)NH} + 31 \text{H}_2\text{O} \cdot \text{H}_3\text{O}^+$	51.9	-80.0
Intra-molecular amide formation via 1,3[H]-transfer		
$\text{HC(OH)NH}(\text{g}) \rightarrow \text{HC(O)NH}_2(\text{g})$	135.5	-57.6
$\text{CH}_3\text{C(OH)NH}(\text{g}) \rightarrow \text{CH}_3\text{C(O)NH}_2(\text{g})$	127.6	-57.1
$\text{HC(OH)NH} + 31 \text{H}_2\text{O} \cdot \text{H}_3\text{O}^+ \rightarrow \text{HC(O)NH}_2 + 31 \text{H}_2\text{O} \cdot \text{H}_3\text{O}^+$	168.8	-81.5
$\text{CH}_3\text{C(OH)NH} + 31 \text{H}_2\text{O} \cdot \text{H}_3\text{O}^+ \rightarrow \text{CH}_3\text{C(O)NH}_2 + 31 \text{H}_2\text{O} \cdot \text{H}_3\text{O}^+$	141.5	-90.1
Inter-molecular amide formation via protonation/deprotonation		
$\text{HC(OH)NH} + 31 \text{H}_2\text{O} \cdot \text{H}_3\text{O}^+ \rightarrow \text{HC(OH)NH}_2^+ + 32 \text{H}_2\text{O}$	1.6	-75.5
$\text{HC(OH)NH}_2^+ + 32 \text{H}_2\text{O} \rightarrow \text{HC(O)NH}_2 + 31 \text{H}_2\text{O} \cdot \text{H}_3\text{O}^+$	5.8	-4.83
$\text{CH}_3\text{C(OH)NH}_2^+ + 32 \text{H}_2\text{O} \rightarrow \text{CH}_3\text{C(O)NH}_2 + 31 \text{H}_2\text{O} \cdot \text{H}_3\text{O}^+$		

Table 2: Barrier heights, E^\ddagger , and reaction enthalpies $\Delta_r H$ (0 K) / kJ mol⁻¹

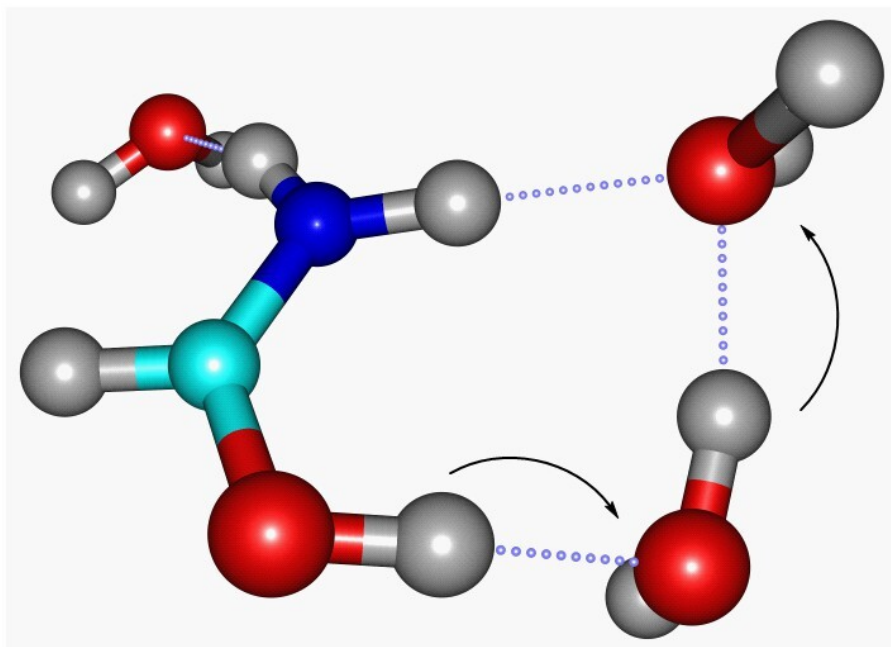


Fig. 8: Intermolecular $\text{HC(OH)=NH} \rightarrow \text{HC(O)NH}_2$

the unfortunately named cyanamide, or amino cyanide $\text{H}_2\text{NC}\equiv\text{N}$, in the hot molecular core G10.47+0.03 and outline three possible fates, degradation to $\text{H}_2\text{N}^\bullet + \text{CN}^\bullet$ by cosmic rays and high-energy photons or by ion–neutral reactions: $\text{H}_2\text{NC}\equiv\text{N} + \text{H}_3^+ \longrightarrow \text{H}_2\text{NC}=\text{NH}^+ + \text{H}_2$. Auto-catalytic addition of water on ice-grains, as per *this work*, would lead to the formation of carbonyl diamide, $\text{OC(NH}_2)_2$, better known as urea, which has been detected previously [53].

In an extensive computational study by Slate et al. [54] into urea formation in the ISM they concluded that closed shell reactions had prohibitive barriers but that a route involving charged species was feasible except that their starting point involved iso-cyanic acid $\text{HN}=\text{C}=\text{O}$ with protonation at the O-atom followed by addition of ammonia and subsequent deprotonation; a somewhat more complex sequence than that envisaged here but nevertheless comparable. Previously Brigiano et al. had considered ion–molecule, neutral–neutral and radical reactions leading to the formation of urea but only in the gas-phase [55].

5 Conclusion

The auto-catalytic addition of water to $\text{RC}\equiv\text{N}$ triple bonds is shown to be a credible process on water clusters which are impacted by hydrons H^+ . The high mobility of the hydron through the cluster leads to the initial reactive

step, protonation at the N-atom in a facile manner. This effectively transforms a bimolecular reaction into a unimolecular process — thus removing the ‘collisional handicap’ which hampers all gas-phase reactions in the interstellar medium.

Subsequent attack by water at carbon and abstraction of H⁺ yields the hydroxy imine RC(OH)NH which can then undergo a 1,3[H]-transfer reaction either intra-molecularly or inter-molecularly to the amide RC(O)NH₂. Quantum-mechanical tunnelling plays a key role in these processes.

The recent review by Woon with its stress on the need to pay more attention to cation–ice reactions is shown to be prescient and his call for experimental confirmation timely. [28]

ORCID

Boutheïna Kerkeni: [0000-0002-5762-5058](https://orcid.org/0000-0002-5762-5058)

John M. Simmie: [0000-0003-0714-7956](https://orcid.org/0000-0003-0714-7956)

Acknowledgement

JMS and BK thank the Irish Centre for High-End Computing, ICHEC, for the provision of computational resources (projects: nuig02, ngche102c, ngche115c) The assistance by David Ferro-Costas (Univ. Santiago de Compostela), author of Pilgrim, is gratefully acknowledged.

References

- [1] Kolesníková L, Belloche A, Koucký J, Alonso ER, Garrod RT, Luková K, Menten KM, Müller HSP, Kania P, Urban Š. Laboratory rotational spectroscopy of acrylamide and search for acrylamide and propionamide towards Sgr B2(N) with ALMA. *A & A* 2021;659:A111
- [2] Ligterink NFW, Ahmadi A, Luitel B, Coutens A, Calcutt H, Tychoniec L, Linnartz H, Jørgensen JK, Garrod RT, Bouwman J. The prebiotic molecular inventory of Serpens SMM1: II. The building blocks of peptide chains. *ACS Earth Space Chem* 2022;6:455-467.
- [3] Adande GR, Woolf NJ, Ziurys LM. Observations of Interstellar Formamide: Availability of a Prebiotic Precursor in the Galactic Habitable Zone. *Astrobiol* 2013;13:439–453.
- [4] McGuire BA. 2021 Census of Interstellar, Circumstellar, Extragalactic, Protoplanetary Disk, and Exoplanetary Molecules. *Astro J* 2022;259:30.
- [5] Schuessler C, Remijan A, Xue C, Carder J, Scolati H, McGuire B. Searching for Propionamide (C₂H₅CONH₂) Toward Sagittarius B2 at Centimeter Wavelengths. *arXiv:2208.05823*
- [6] Barone V, Latouche C, Skouteris D, Vazart F, Balucani N, Ceccarelli C, Lefloch B. Gas-phase formation of the prebiotic molecule formamide: insights from new quantum computations. *MNRAS* 2015;453:L31–L35

- [7] Skouteris D, Vazart F, Ceccarelli C, Balucani N, Puzzarini C, Barone V. New quantum chemical computations of formamide deuteration support gas-phase formation of this prebiotic molecule. *MNRAS* 2017;468:L1–L5.
- [8] Song L, Kästner J. Formation of the prebiotic molecule NH_2CHO on astronomical amorphous solid water surfaces: accurate tunneling rate calculations. *Phys Chem Chem Phys*, 2016;18:29278
- [9] Douglas KM, Lucas D, Walsh C, West NA, Blitz MA, Heard DE. The gas-phase reaction of NH_2 with formaldehyde (eCH_2O) is not a source of formamide (NH_2CHO) in interstellar environments. *arXiv:2208.12658*
- [10] Fedoseev G, Chang K-J, van Dishoeck EF, Ioppolo S, Linnartz H. Simultaneous hydrogenation and UV-photolysis experiments of NO in CO-rich interstellar ice analogues; linking HNC, OCN^- , NH_2CHO , and NH_2OH . *MNRAS* 2016;460:4297–4309.
- [11] Jones BM, Bennett CJ, Kaiser RI. Mechanistical studies on the production of formamide (H_2NCHO) within interstellar ice analogs. *Astro J* 2011;734:78.
- [12] Thripati S, Ramabhadran RO. Pathways for the Formation of Formamide, a Prebiotic Biomonomer: Metal-Ions in Interstellar Gas-Phase Chemistry. *J Phys Chem A* 2021;125: 3457–3472
- [13] Chuang KJ, Jäger C, Krasnokutski SA, Fulvio D, Henning T. Formation of the simplest amide in molecular clouds: formamide (NH_2CHO) and its derivatives in H_2O -rich and CO-rich interstellar ice analogs upon VUV irradiation. *Astro J* 2022; 933:107. *arXiv:2206.10470v*
- [14] Lee C-F, Codella C, Ceccarelli C, López-Sepulcre A. Stratified Distribution of Organic Molecules at the Planet-Formation Scale in the HH 212 Disk Atmosphere. *arXiv:2208.10693*
- [15] Cordiner MA, Remijan AJ, Boissier J, Milam SN, Mumma MJ, Charnley SB, Paganini L, Villanueva G, Bockelée-Morvan D, Kuan Y-J, et al Mapping the release of volatiles in the inner comae of comets C/2012 F6 (Lemmon) and C/2012 S1 (ISON) using the Atacama large millimeter/submillimeter array. *Astrophys J* 2014;792:L2
- [16] Loomis RA, Cleeves LI, Oberg KI, Aikawa Y, Bergner J, Furuya K, Guzman VV, Walsh C. The Distribution and Excitation of CH_3CN in a Solar Nebula Analog. *Astro J* 2018;859:131.
- [17] Colzi L, Rivilla VM, Beltrán MT, Jiménez-Serra I, Mininni C, Melosso M, Cesaroni R, Fontani F, Lorenzani A, Sanchez-Monge A, et al. The GUAPOS project ii. A comprehensive study of peptide-like bond molecules. *A & A* 2021;653.
- [18] Kalvāns K, Silsbee K. Icy molecule desorption in interstellar grain collisions. *MNRAS* 2022;515:785–794.
- [19] Minissale M, Aikawa Y, Bergin E, et al. Thermal Desorption of Interstellar Ices: A Review on the Controlling Parameters and Their Implications from Snowlines to Chemical Complexity. *CS Earth & Spac Chem* 2022;6:59–630.

- [20] Darla N, Sharma D, Sitha S. Formation of Formamide from HCN + H₂O: A Computational Study on the Roles of a Second H₂O as a Catalyst, as a Spectator, and as a Reactant. *J Phys Chem A* 2020;124:165–175
- [21] Rimola A, Skouteris D, Balucani N, Ceccarelli C, Enrique-Romero J, Taquet V, Ugliengo P. Can Formamide Be Formed on Interstellar Ice? An Atomistic Perspective. *ACS Earth Space Chem* 2018;2:720–734
- [22] Bulak M, Paardekooper DM, Fedoseev G, Linnartz H. Photolysis of acetonitrile in a water-rich ice as a source of complex organic molecules: CH₃CN and H₂O : CH₃CN ices. *A & A* 2021;647:A82
- [23] Simmie JM. C₂H₅NO Isomers: From Acetamide to 1,2-Oxazetidine and Beyond. *J Phys Chem A* 2022;126:924–936.
- [24] Wootten A, Mangum JG, Turner BE, Bogey M, Boulanger F, Combes F, Encrenaz PJ, Gerin M. Detection of Interstellar H₃O⁺: A Confirming Line. *Astrophys J* 1991;380:L79.
- [25] Tak FD, Aalto S, Meijerink R. Detection of extragalactic H₃O⁺. *A & A* 2007;477:5–8.
- [26] Moon ES, Kang H, Oba Y, Watanabe N, Kouchi A. Direct Evidence for Ammonium Ion Formation in Ice Through Ultraviolet-Induced Acid Base Reaction of NH₃ with H₃O⁺. *Astrophys J* 2010;713:906.
- [27] Lee DH, Kang H. Proton Transport and Related Chemical Processes of Ice. *J Chem Phys B* 2021;125:8270–8281
- [28] Woon DE. Quantum chemical cluster studies of cation-ice reactions for astrochemical applications: Seeking experimental confirmation. *Accts Chem Res* 2021;54:490-497.
- [29] Martinez R, Agnihotri AN, Boduch P, Domaracka A, Fulvio D, Palumbo ME, Rothard H, Strazzulla G. Production of Hydronium Ion (H₃O⁺) and Protonated Water Clusters (H₂O_{*n*} · H⁺) after Energetic Bombardment of Water Ice in Astrophysical Environments. *J Phys Chem A* 2019; 123: 8001–8008.
- [30] Ziurys LM, Turner BE. Detection of interstellar vibrationally excited HCN. *Ap J* 1986;302:L31
- [31] Schilke P, Walmsley CM, Henkel C, Millar TJ. Protonated HCN in molecular clouds. *A & A* 1991;247:487.
- [32] Quénard D, Vastel C, Ceccarelli C, Hily-Blant P, Lefloch B, Bachiller R. Detection of the HC₃NH⁺ and HCNH⁺ ions in the L1544 pre-stellar core. *MNRAS* 2017;470:3194
- [33] Cravens TE, Robertson IP, Waite JH, Yelle RV, Kasprzak WT, Keller CN, Ledvina SA, Nieman HB, Luhmann JG, McNutt RL, Ip W-H, de la Haye V, Mueller-Wodarg I, Wahlund J-E, Anicich VG, Vuitton V. Composition of Titan's ionosphere. *Geophys Res Lett* 2006;33:L07105
- [34] Fontani F, Colzi L, Redaelli E, Sipilä O, Caselli P. First survey of HCNH⁺ in high-mass star-forming cloud cores. *A & A* 201;651:A94.
- [35] Marimuthu AN, Huis in't Veld F, Thorwirth S, Redlich B, Brünken S. Infrared predissociation spectroscopy of protonated methyl cyanide, CH₃CNH⁺. *J Mol Spectros* 2021;379:

- [36] Lee DH, Choi CH, Choi TH, Sung BJ, Kang H. Asymmetric transport mechanisms of hydronium and hydroxide ions in amorphous solid water: Hydroxide goes Brownian while hydronium hops. *J Phys Chem Letts* 2014;5:2568-2572.
- [37] Krasnokutski SA, Chuang KJ, Jager C, Ueberschaar N, Henning T. A pathway to peptides in space through the condensation of atomic carbon. *Nature Astronomy* 2022;6:381–386.
- [38] Canepa C. A Model Study on the Dynamics of the Amino Acid Content in Micrometeoroids during Atmospheric Entry. *Chemistry* 2020;2:918–936.
- [39] Gaussian 16, Revision C.01, Frisch, M. J.; Trucks, G. W.; Schlegel, H. B.; Scuseria, G. E.; Robb, M. A.; Cheeseman, J. R.; Scalmani, G.; Barone, V.; Petersson, G. A.; Nakatsuji, H.; Li, X.; Caricato, M.; Marenich, A. V.; Bloino, J.; Janesko, B. G.; Gomperts, R.; Mennucci, B.; Hratchian, H. P.; Ortiz, J. V.; Izmaylov, A. F.; Sonnenberg, J. L.; Williams-Young, D.; Ding, F.; Lipparini, F.; Egidi, F.; Goings, J.; Peng, B.; Petrone, A.; Henderson, T.; Ranasinghe, D.; Zakrzewski, V. G.; Gao, J.; Rega, N.; Zheng, G.; Liang, W.; Hada, M.; Ehara, M.; Toyota, K.; Fukuda, R.; Hasegawa, J.; Ishida, M.; Nakajima, T.; Honda, Y.; Kitao, O.; Nakai, H.; Vreven, T.; Throssell, K.; Montgomery, J. A., Jr.; Peralta, J. E.; Ogliaro, F.; Bearpark, M. J.; Heyd, J. J.; Brothers, E. N.; Kudin, K. N.; Staroverov, V. N.; Keith, T. A.; Kobayashi, R.; Normand, J.; Raghavachari, K.; Rendell, A. P.; Burant, J. C.; Iyengar, S. S.; Tomasi, J.; Cossi, M.; Millam, J. M.; Klene, M.; Adamo, C.; Cammi, R.; Ochterski, J. W.; Martin, R. L.; Morokuma, K.; Farkas, O.; Foresman, J. B.; Fox, D. J. Gaussian, Inc., Wallingford CT, 2016.
- [40] Chai J-D, Head-Gordon M. Long-range corrected hybrid density functionals with damped atom–atom dispersion corrections. *PCCP* 2008;10:6615–6620.
- [41] Hratchian HP, Schlegel HB. Accurate reaction paths using a Hessian based predictor–corrector integrator. *J Chem Phys* 2004;120:9918.
- [42] Hratchian HP, Schlegel HB. Using Hessian Updating To Increase the Efficiency of a Hessian Based Predictor-Corrector Reaction Path Following Method. *JCTC* 2005;1:61–69.
- [43] Page M, McIver Jr JW. On evaluating the reaction path Hamiltonian. *J Chem Phys* 1988;88:922–935.
- [44] Liu Y-P, Lynch GC, Truong TN, Lu D-H, Truhlar DG. Molecular Modelling of the Kinetic Isotope Effect for the [1,5]-Sigmatropic Rearrangement of cis-1,3-Pentadiene. *JACS* 1993;115:2408.
- [45] Wonchoba SE, Hu W-P, Truhlar DG. Theoretical and Computational Approaches to Interface Phenomena, eds. Sellers HL, Golab JT. Plenum, New York, 1994. Pp. 1 Reaction Path Approach to Dynamics at a Gas-Solid Interface: Quantum Tunnelling Effects for an Adatom on a Non-Rigid Metallic Surface.
- [46] PILGRIM v2021.5 <https://github.com/cathedralpkg/pilgrim>
- [47] Enrique-Romero J, Rimola A, Ceccarelli C, Ugliengo P, Balucani N,

- Skouteris D. Reactivity of HCO with CH₃ and NH₂ on Water Ice Surfaces. A Comprehensive Accurate Quantum Chemistry Study. ACS Earth Space Chem 2019;3:2158–2170
- [48] Hunter EP, Lias SG. Evaluated Gas Phase Basicities and Proton Affinities of Molecules: An Update, J Phys Chem Ref Data, 1998; 27: 413–656.
- [49] Ferro-Costas D, Truhlar DG, Fernández-Ramos A. Pilgrim: A thermal rate constant calculator and a chemical kinetics simulator. Comp Phys Comms 2020;256:107457
- [50] Concepción JG, Jiménez-Serra I, Corchado JC, Rivilla VM, Martín-Pintado J. The Origin of the E/Z Isomer Ratio of Imines in the Interstellar Medium. Ap J L 2021;912:L6
- [51] Bianchi E, Ceccarelli C, Codella C, SOLIS XV. CH₃CN deuteration in the Class I hot corino. A & A 2022; 662:A103.
- [52] Manna A, Pal S. Detection of interstellar cyanamide (NH₂CN) towards the hot molecular core G10.47+0.03. arXiv:2207.04877
- [53] Belloche A, Garrod RT, Müller HSP, Menten KM, Medvedev I, Thomas J, Kisiel Z, Re-exploring Molecular Complexity with ALMA (ReMoCA): interstellar detection of urea. A & A;2019:628,A10. *See also* A & A 2020;637:C4.
- [54] Slate ECS, Barker R, Euesden RT, Revels MR, Meijer AJHM. Computational studies into urea formation in the interstellar medium. MNRAS 2020;497:5413–5420
- [55] Brigiano FS, Jeanvoine Y, Largo A, Spezia R. The formation of urea in space I. Ion-molecule, neutral-neutral, and radical gas-phase reactions. A & A 2018;610:A26.